The Effect of Curcumin on the Stability of Aβ Dimers

ARTICLE *in* THE JOURNAL OF PHYSICAL CHEMISTRY B · JUNE 2012

Impact Factor: 3.3 · DOI: 10.1021/jp3034209 · Source: PubMed

5 AUTHORS, INCLUDING:

See-Wing Chiu
University of Illinois, Urbana-Champaign
47 PUBLICATIONS **1,818** CITATIONS
SEE PROFILE

Jerome BENOIT
ReZoZeR
15 PUBLICATIONS **101** CITATIONS
SEE PROFILE

Lock Yue Chew
Nanyang Technological University
65 PUBLICATIONS **335** CITATIONS
SEE PROFILE

Yuguang Mu
Nanyang Technological University
119 PUBLICATIONS **2,797** CITATIONS
SEE PROFILE

THE JOURNAL OF PHYSICAL CHEMISTRY B

Article

pubs.acs.org/JPCB

The Effect of Curcumin on the Stability of Aβ Dimers

Li Na Zhao,[†] See-Wing Chiu,[‡] Jérôme Benoit,[†] Lock Yue Chew,*[,†] and Yuguang Mu*[,§]

[†]School of Physical and Mathematical Sciences, Nanyang Technological University

[‡] Beckman Institute, University of Illinois, Urbana, Illinois

[§]School of Biological Sciences, Nanyang Technological University, 60 Nanyang Drive, Singapore

Supporting Information

ABSTRACT: Aβ oligomers are potential targets for the diagnosis and therapy of Alzheimer's disease (AD). On the other hand, the molecule curcumin has been shown to possess significant therapeutic potential in many areas. In this paper, we use all-atom explicit solvent molecular dynamics simulations to study the effect of curcumin on the stability of Aβ amyloid protein oligomers. We observed that curcumin decreases the β-sheet secondary structural content within the Aβ oligomers without reducing the contacts between the monomers. The breaking of the β-sheet is found to be preceded by a deformation of the β-sheet structure due to hydrophobic interaction from the nearby curcumin. Furthermore, the π-stacking interaction between curcumin (keto ring and enol ring) and the aromatic residues of Aβ, which exists throughout the simulations, has also contributed to the diminishing of the β-sheet structure. Our analysis of the underwrapped amide−carbonyl hydrogen bonds reveals several stable dehydrons of the oligomer, especially the dehydron pair 34L and 41I, which curcumin tends to hover over. We have examined the paths of curcumin on the Aβ proteins and determined the common routes where curcumin lingers as it traverses around the Aβ. In consequence, our study has provided a detailed interaction picture between curcumin and the Aβ oligomers.

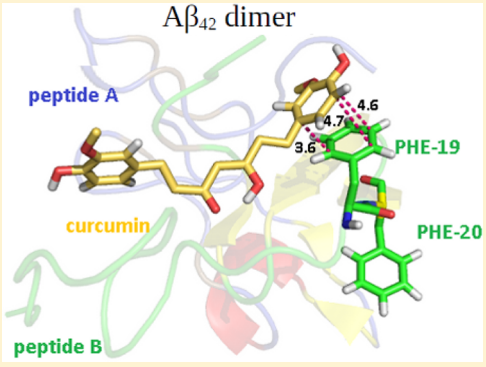

INTRODUCTION

The Aβ peptide has long been believed to be a potential target for combating Alzheimer's Disease (AD).[1] The aggregation of Aβ with the formation of toxic oligomers is one of the central pathological pathways[2] that causes AD. The toxicity mechanism of Aβ oligomers appears through a change in the membrane receptors' functions,[3] creation of pores in the membrane,[4−7] alteration of ionic homeostasis,[8,9] modification of DNA structure,[10] and formation of a metal-Aβ complex that induces oxidative stress.[11,12] Small molecules, such as resveratrol,[13] mitoxantrone, and pixantrone,[14] derivatives of Congo Red,[15] curcumin, and other compounds, such as 1,4-naphthoquinon-2-yl-L-tryptophan (NQTrp),[16] have been shown to inhibit the process of Aβ aggregation. They are also potential labeling agents for the diagnosis and monitoring of AD.[17]

Curcumin, which is usually extracted from turmeric and comes with a major polyphenol component, has served as traditional medicine for centuries and has been used as a natural food additive. Curcumin and its derivatives have also been shown to possess significant therapeutic potential as antioxidants and anticarcinogens, with its anti-inflammatory effect[18] well suited for the healing of skin wounds. It is suggested that incorporating curcumin into the cell membrane can induce segmental ordering of the membrane[19] and modulate diverse membrane proteins by means of the bilayer-mediated mechanism.[20] The increasing attention on curcumin results from its observed therapeutic potential and intrinsic nontoxicity.

Recent research has uncovered a strong connection between curcumin and AD. For example, a regular diet of curcumin can reduce the risk of AD.[21] Curcumin is also found to regulate the production of Aβ by indirectly suppressing the expression of presenilin 1, which is related to γ secretase and the generation of Aβ.[22] With its unique physicochemical properties, curcumin can pass the blood-brain barrier and interact with Aβ.[23] Curcumin may also bind directly to small Aβ oligomers to block aggregation, hence lowering or reversing Aβ oligomer toxicity by disrupting the development of plaques in vitro and in vivo.[10,12,24,25] Curcumin and its derivatives can rescue functional failures, such as spontaneous firing inhibition of the hippocampal neurons, and long-term potentiation damage induced by the Aβ oligomers.[26,27] Furthermore, curcumin may protect the neuron from Aβ insult and degeneration.[28,29] However, research has indicated that the neuronal protective effect is concentration-dependent and high dosages of curcumin may result in cell damage in the presence of Cu(II).[11] Some curcumin derivatives have also been used as radioligands for Aβ plaque imaging due to their binding affinities toward the $Aβ_{1-42}$ aggregate.[30] Despite the extensive studies being done and

Received: April 10, 2012
Revised: June 6, 2012
Published: June 11, 2012

several mechanisms being proposed[31] on the inhibitory effects of curcumin in recent decades, the detailed mechanism of how curcumin interacts with the Aβ oligomers still awaits further identification and elucidation.

Curcumin consists of two aromatic end groups with a linker region in the middle. Early studies have shown that the predominant tautomer is β-diketone in aqueous environment.[32] However, recent X-ray and NMR studies have found that curcumin tends to exist in solution as an enol−keto tautomer rather than a β-diketone tautomer[33,34] in lieu of the more stable planar structure of the former and also due to energy consideration. Hence, in this article, we focus our analysis on the keto−enol form of curcumin. Nonetheless, we have found that the simulation results from the β-diketone tautomer form of curcumin are essentially the same as those of the keto−enol form. The chemical structure of curcumin is displayed in Figure 1.

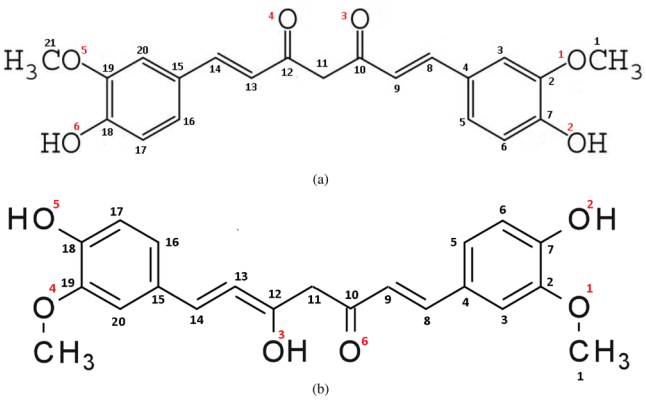

Figure 1. The chemical structure of curcumin: (a) β-diketone tautomer, and (b) keto−enol tautomer. Note that the carbon atoms are labeled by numbers in black and oxygen atoms in red.

METHODS AND SIMULATION SETUP

The initial structure of Aβ_{42}, whose sequence is DAEFRHDSGY$_{10}$ EVHHQKLVFF$_{20}$ AEDVGSNKGA$_{30}$ IIGLMVGGVVIA$_{42}$, was taken from model 1 of the Protein Data Bank (PDB) ID: 1IYT.[35] The pK_a values of the titratable residues was calculated by the H++ server[36,37] (see Supporting Information Table S1). The default internal and external dielectric constants of 6 and 80 respectively, were used in the calculation. The ionic strength was set to 0.1 M with pH 7. The structure of the small curcumin molecule was obtained from the ZINC database[38] (see Figure 1). The initial topology and force field parameters of curcumin was generated in the PRODRG2 Server[39] (see Supporting Information Table S2). The protein and curcumin are represented by the GROMOS96 53a6 force field, which is able to model the Aβ structural propensities in agreement with experimental NMR results.[40]

In our simulations, all bonds were constrained using the linear constraint solver (LINCS)[41] algorithm with a 2 fs integration time step. The temperature was kept at 300 K using the Nosé−Hoover coupling scheme.[42,43] A semi-isotropic pressure coupling at 1 bar by means of a Parrinello−Rahman barostat with a coupling constant of 2 ps was used in the pressure ensemble. The van der Waals cutoff was set to 1.0 nm. the particle mesh Ewald method[44] was used for electrostatic interaction with a fourth-order interpolation and a Fourier grid spacing of 0.16 nm. The preparation steps, simulations, and analysis were performed using facilities within the GROMACS package. The docking was conducted using Autodocktools.[45] PyMOL[46] and VMD[47] were used to visualize the molecular structures. Additional analysis and visualization were assisted by WRAPPA,[48] MATLAB, OriginPro, and some in-house scripts.

Our first set of simulations was performed on a single Aβ peptide in a cubic box of dimensions 52.60 Å × 52.60 Å × 52.60 Å for 200 ns. The box was filled with 5582 water molecules, 13 Na^+ ions, and 11 Cl^- ions to neutralize the system. The final Aβ peptide structure was taken as the initial structure for the subsequent simulations.

In our second set of simulations, 5 Aβ of the final conformation from the first set were used and aligned parallel in a cubic box of dimensions 166.86 Å × 46.87 Å × 46.87 Å. The center of mass of each peptide was placed at (23.43, 23.43, 23.43), (53.43, 23.43, 23.43), (83.43, 23.43, 23.43), (113.43, 23.43, 23.43), and (143.43, 23.43, 23.43), and the peptides were labeled as chains A, B, C, D, and E, respectively. The simulation was conducted for a period of 1000 ns.

In our third set of simulations, we took the dimer that was formed by peptides A and B at the end of the second simulation (see Supporting Information Figure S1, which is labeled as model 0 or M0) to be used as initial structure for docking. AutoDock 4[45] was then employed to dock the curcumin (β-diketone tautomer) onto the preformed dimer. During the docking simulations, the gasteiger charge was computed, and Autodock type was assigned to the curcumin, and 12 active torsion angles (rotable bonds) were defined as the flexible parts. To explore the possible binding sites, the whole dimer was treated as a blind docking area. The docking space was defined via the dimensions 106 × 102 × 126, with an autodock default grid spacing of 0.375 Å. The grid box was centered on the dimer and covered the whole of the dimer. Ten complex conformations (dimer and curcumin) with the lowest docking energy from the most populated clusters were taken as initial structures for further MD simulations. We labeled these conformations as M1−M10. Similarly, we performed docking for the keto−enol tautomer form of curcumin, and 10 complex structures with lowest docking energy were chosen and labeled as M11−M20.

During the subsequent MD simulations, each of the M0−M20 models was put in the center of a cubic box with dimensions 62.14 Å × 62.14 Å × 62.14 Å. All the conformations were then solvated using the SPC water model,[49] with 18 Na^+ ions and 14 CL^- ions added to neutralize the system. This was followed by 500 ns of MD simulation for each system.

RESULTS

Curcumin as β-Sheet Breaker. In models 1 and 2, curcumin is observed to initially bind with both peptides A and B. In model 5 (model 10), curcumin is found to bind with His-14, Leu-17, and Phe-19 from peptide B (peptide A) after docking. The detailed information about these models can be found in Supporting Information Figures S2, S3, and Table S3. The number of residues that adopts the β-sheet conformation in the absence/presence of curcumin and the secondary structure evolution was monitored and is shown in the Supporting Information (see Figures S4, S5 and S6). Without curcumin (model 0), the number of residues with β-sheet structure is found to increase for both peptides A and B. The number of residues which form β-sheet structure in peptide A is

dx.doi.org/10.1021/jp3034209 | J. Phys. Chem. B 2012, 116, 7428−7435

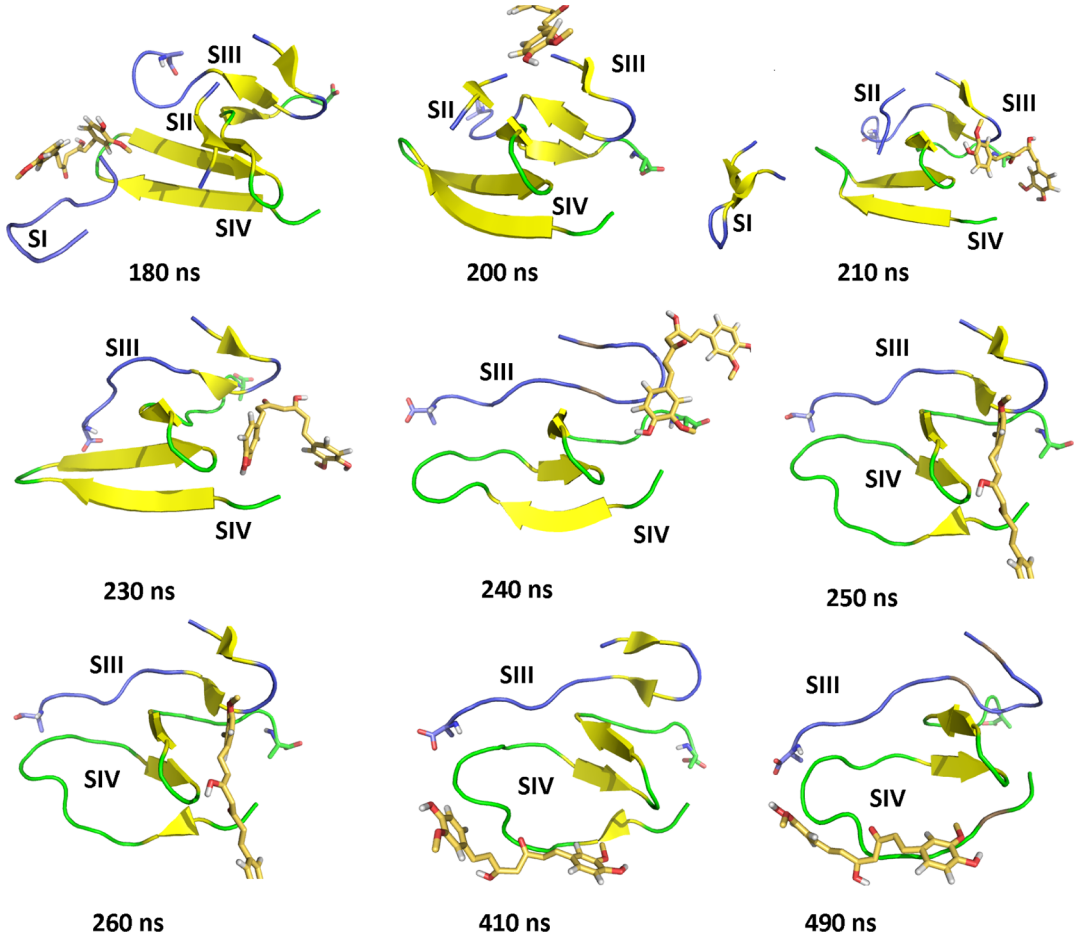

Figure 2. Snapshots of curcumin acting as β-sheet breaker. Sevearl segments of the Aβ peptides were shown for clarity. The blue loop represents residues from peptide A; green loop represents residues from peptide B. The C-termini (namely, residue Val-42) are shown as sticks and colored blue for peptide A and green for peptide B. The molecule curcumin is represented by golden sticks and colored by element.

relatively stable, from 6 in the beginning to 8 at the end of the simulation. Conversely, there is an obvious increase in the number of residues with β-sheet structure in peptide B, from 14 in the beginning to 21 at the end of the simulation, and most of the β-sheet segments are found to be well maintained. In models with curcumin, the β-sheet structure is found to collapse and reorganize. We found that the presence of curcumin generally destabilizes the β-sheet structure. The average number of residues of Aβ dimer that adopts the β-sheet structure in the absence of curcumin is around 27.16. On the other hand, the average number of residues that forms β-sheet structure in the presence of curcumin is around 21.48. Hence, curcumin induces a 21% reduction in the number of β-sheet residues. Note that the average here was performed with respect to time, and for the case with curcumin, a further average over the time-averaged β-sheet content over the 10 models was carried out (see Supporting Information Figure S4). The details of the secondary structure propensity of Aβ residues in the presence and absence of curcumin are illustrated in Supporting Information Figure S6.

The number of contacts, that is, the number of heavy atom pairs whose distance is smaller than 0.6 nm between peptides A and B, was also calculated. A weakly negative correlation is found between the number of contacts and the number of β-sheet residues, with an average Pearson correlation coefficient of −0.13 for all models.

To further examine this phenomenon, we had also checked on the protein segment 17−42, which was reported to form well-ordered Aβ fibrils. This segment is also known to stay in the hydrophobic core of the membranes.[50,51] The correlation between the number of β-sheet residues and the number of contacts between peptides A and B within the segment of 17−42 is also slightly negative, with an average Pearson coefficient of −0.22. These results indicate that although the number of β-sheet residues reduces in the presence of curcumin, it is not necessary for the contacts between the two monomers to decrease.

The role of curcumin as a β-sheet breaker is clearly demonstrated through the evolution of the secondary structures within a selected trajectory (see Figure 2). The snapshots of secondary structures of four segments, SI: $_{3}$E−$_{11}$E; SII: $_{17}$L−$_{20}$F; SIII: $_{30}$A−$_{42}$V all from peptide A; and SIV: $_{17}$L−$_{42}$V from peptide B, are illustrated. At 180 ns, curcumin disrupts the β-sheet structure of SI due to its proximity, which can be perceived through the reemergence of the antiparallel β-sheet at SI as curcumin departs from the region. On the other hand, a close scrutiny on SII shows that its β-sheet structure has been transformed to a loop at 200 ns, which results from the indirect influence of the nearby curcumin. Since there is no change in the secondary structure contents of SI and SII after 210 ns, these segments are not displayed in the following snapshots of Figure 2. It is observed that curcumin destroys β-sheets by

dx.doi.org/10.1021/jp3034209 | J. Phys. Chem. B 2012, 116, 7428−7435

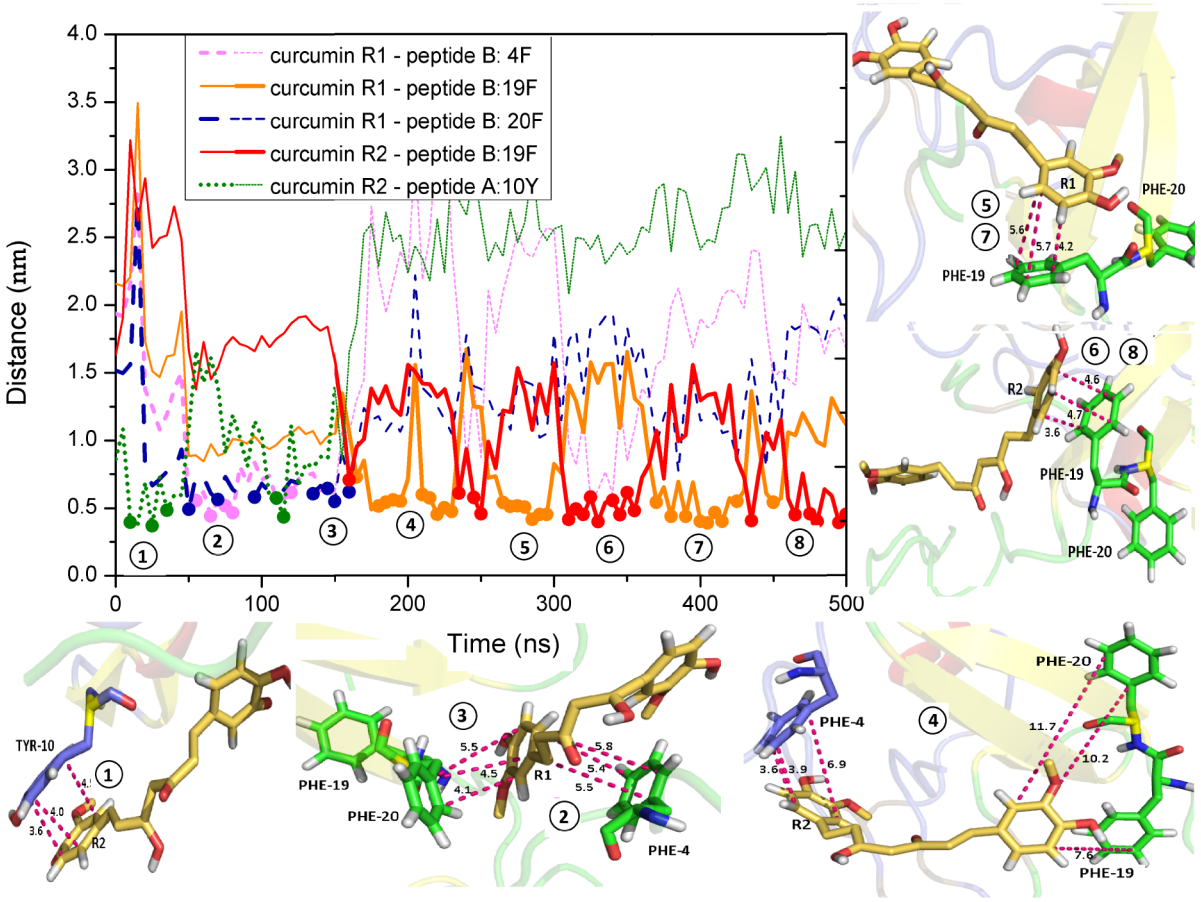

Figure 3. A plot of the center of mass distance between the ring of curcumin and the aromatic ring of Aβ residues. The minimum distance is indicated by heavy dots with numbers. Representative snapshots of π-stacking between the ring of curcumin and the aromatic residues of peptide A and B are given (the aromatic ring is colored blue for peptide A and green for peptide B). The red dash highlights the distance between the atoms (unit: Å). The residues on Aβ are represented as sticks and colored by element (O, red; H, gray; N, blue); the C_α sitting on the β-sheet are yellow. The molecule curcumin is represented as a stick (C, yellow; O, red; H, gray).

twisting and bending the sheet. Such a deformation of the β-sheet is observed in SIV at 200 ns. This leads to two residues, 24V and 27N, from each strand detaching from the β-strands and joining the linking loop of the β-sheets at around 210 ns. It is also observed that the presence of curcumin near SIII from 230 to 240 ns serves to temporarily unfold the β hairpin near the region. Then at around 250 ns, the β hairpin at SIII reappears as the curcumin moves away. In the meantime, the curcumin molecule travels close to SIV, which further destabilizes the β-sheet structure there and modifies it into an unstructured loop until the end of our simulations. It is important to note that such destabilization effects are not observed in the simulation on M0. In fact, we have noticed similar patterns in the curcumin-Aβ interactions in other trajectories. In some of these trajectories, β-sheets are detected to quickly restore after curcumin leaves the interaction region. The overall β-sheet collapses, however, are not as obvious as those shown in Figure 2. We have also uncovered that curcumin is able to make hydrogen bonds with Aβ. More specifically, the enol and the phenolic groups (the −OH on the aromatic rings) of curcumin can act as donor/acceptor. The −OH group of curcumin has more than twice the chance of forming hydrogen bonds with Aβ than the methoxy group (the percentage of hydrogen bonds being formed from −OH and −OCH3 is found to be 50% and 20%, respectively).[52]

π-Stacking between Curcumin and Aβ. The $\pi-\pi$ nonbonded attractive interaction is prevalent among aromatic residues, DNA, RNA, polyphenol components, and carbon nanotubes in biomedical applications.[53−58] This interaction is known to contribute to the stability of tertiary structures of macromolecules. It has served to control molecular recognition in some aromatic substituent drugs and is responsible for the enhancement of adsorption affinity and efficiency.[58,59] In this section, we explore the π-stacking between curcumin and Aβ, whose interaction is determined by calculating the ring−ring distance between the residues Tyr, Phe, and His on Aβ, and the two rings on curcumin. The two rings of curcumin were labeled as R1 (keto ring) and R2 (enol ring). Here, we focus mainly on the interaction between pairs of aromatic rings and typically ignore clusters consisting of three or more aromatic rings.

At the beginning of the simulation, π-stacking exists between the R2 of curcumin and the Tyr-10 from peptide A (see position ① of Figure 3). This is followed by the transient tri-π stacking (see positions ② and ③), which is formed among the curcumin R1 ring and the Phe-4 and Phe-20 from peptide B. There is a very short period of time when π-stacking occurs between the Phe-4 from peptide A and the R2 of curcumin (see position ④). Then from 200 ns onward, the R1 and R2 rings of curcumin are observed to interact alternately with the Phe-19 of peptide B (see ⑤−⑧) through π-stacking. Indeed, all the computed trajectories with curcumin presence have shown that

dx.doi.org/10.1021/jp3034209 | J. Phys. Chem. B 2012, 116, 7428−7435

π-stacking occurs very frequently between the rings in curcumin and the aromatic rings in Aβ. Although the $\pi-\pi$ stacking interactions are transient, they contribute indirectly to a reduction in the β-sheet content in the Aβ dimer. In particular, we observe that the residue Phe demonstrates a higher propensity to be involved in such interaction with the rings of curcumin than the residue HIS (see Supporting Information Figure S7).

Dehydron. The concept of dehydron,[60] that is, the under-wrapped amide-carbonyl hydrogen bonds of proteins, is helpful in the design of pharmaceuticals with improved binding affinities.[61,62] Here, we discuss the identification of dehydrons of the Aβ dimer and also our investigation on the interactions of dehydron with curcumin. For each of the 10 models (i.e., M11−M20), we extract the snapshots of dimer plus curcumin structure per 10 ns of each trajectory. This leads to a total of 510 structural snapshots. The program WRAPPA[48] is then used to locate the dehydrons without any consideration of the poorly wrapped C-terminus (Ala-42). Note that we have used a default WRAPPA[48] desolvation domain radius of 6.5 Å as the cutoff distance between the under-wrapped and the well-wrapped amide−carbonyl hydrogen bonds.[63]

Our analysis of all dehydrons has found that the dehydron with a hydrogen bond forming between the amide−carbonyl group of the pair 24V and 27N from peptide B appears in 292 of the 510 structures, whereas that between 24V and 27N from peptide A occurs in 222. A reason for the high frequency of the dehydron pair (24V, 27N) is because 27N is a polar residue. Hence, it prefers to locate on the surface of the protein. Another reason is that the two residues 24V and 27N tend to situate at the end of a strand of antiparallel β-sheet on peptide B, whereas the pair from peptide A participates frequently in the short intermittent antiparallel β-sheet that forms during simulations (see Figure 4a). Incidentally, 28-Lys and 24-Val are noticed to have a high propensity to act as wrapper residues (see Figure 4b).

The second most popular dehydron pair in rank belongs to residues 11E and 15Q, with 157 structures found in peptide A and 110 structures in peptide B. These residues are polar in nature, with residue 15Q tending to be part of a short α-helical structure (see Figure 5). The residue 34L from peptide A and 41I from peptide B with hydrogen bond between them is ranked the third most frequent dehydron pair. This dehydron pair is important because of its frequent interaction with curcumin, which will be discussed in greater detail in the next section.

The characteristics of other dehydrons can be found in Supporting Information Table S4. In summary, the popular dehydrons are listed as follows: (24V, 27N), (11E, 15Q), (34L, 41I) and (28K, 40V), with residues Lys, Val, Ile, and Tyr found to be the most likely neighbors of dehydrons. Scrutinizing the interaction behaviors of curcumin and Aβ, we observed that curcumin tends to stay around several dehydron pairs. More significantly, Figure 5 shows that curcumin spends a minimal amount of time around residues that are not dehydrons.

Nomadism: the Common Routes of Curcumin As It Travels around Aβ. The interaction between curcumin and Aβ is very dynamic. As a consequence, the position of curcumin is not fixed, and the molecule travels around the Aβ. Hence, the word "nomadism" is borrowed to characterize such itinerant behavior of curcumin. By labeling the position of curcumin in each structure through the Aβ residue that is closest to it, the location propensity of curcumin on Aβ was calculated from all

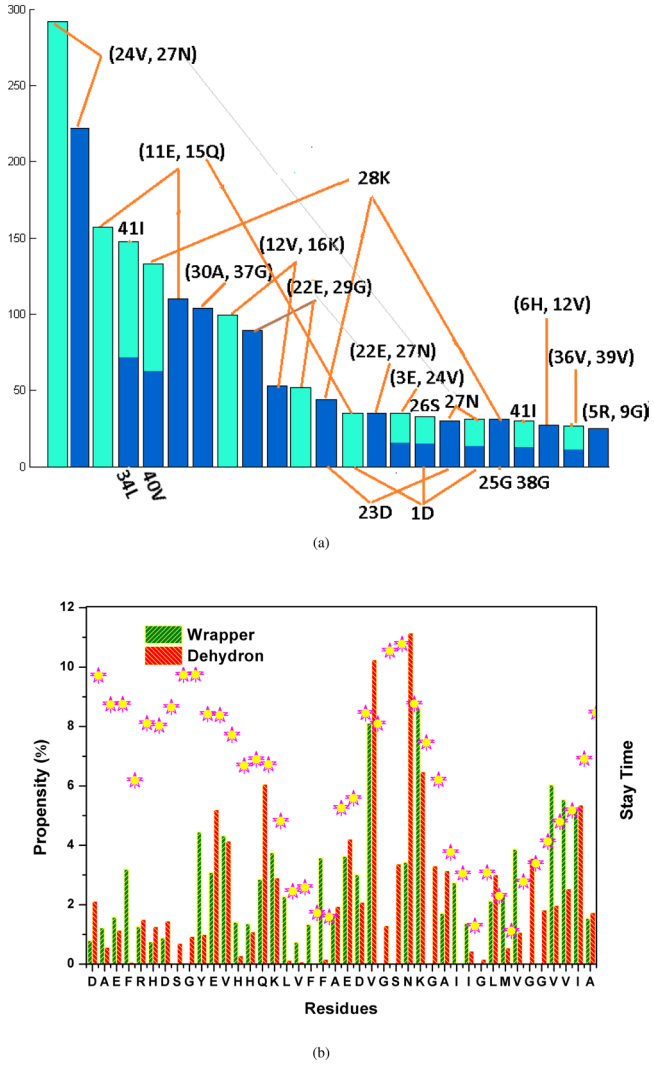

Figure 4. (a) A plot of the number of occurrences of dehydrons in the Aβ dimer. The blue bar indicates that both residues of the dehydrons result from peptide A, and the green bar indicates that both arise from peptide B. The half blue and half green bar indicates that the residue that forms the dehydrons comes from peptide A (blue) and peptide B (green). (b) A plot of the propensity of the Aβ dimer residues to adopt the role of wrapper or dehydron as quantified by the height of the color bar. The time that curcumin spends staying around the Aβ residues is indicated by the scattered maple dots.

the trajectories and is illustrated in Figure 5. Our results show that curcumin tends to stay close to the residues 34-Leu, 22-Glu and the nearby His residues. Indeed, the hydrophobic nature of residues 34-Leu and 32-Ile has rendered them the main recognition and binding sites for the curcumin ligand.[64] The residue histidine is known to act as a binding sites for protein. Here, it is also observed to be involved as a preferred binding site for curcumin.

Curcumin is observed to be rather mobile around the Aβ dimer. We attempted to find patterns in the paths of curcumin as it traverses about the Aβ. The observed patterns turn out to be the common routes of curcumin. A route is made up of steps, and a step is defined as the movement of curcumin from a position close to one residue of Aβ to a position close to another residue. The common routes must be composed of at least four steps and are to be shared by two routes from two different trajectories. By making a pairwise analysis on all 10

dx.doi.org/10.1021/jp3034209 | J. Phys. Chem. B 2012, 116, 7428−7435

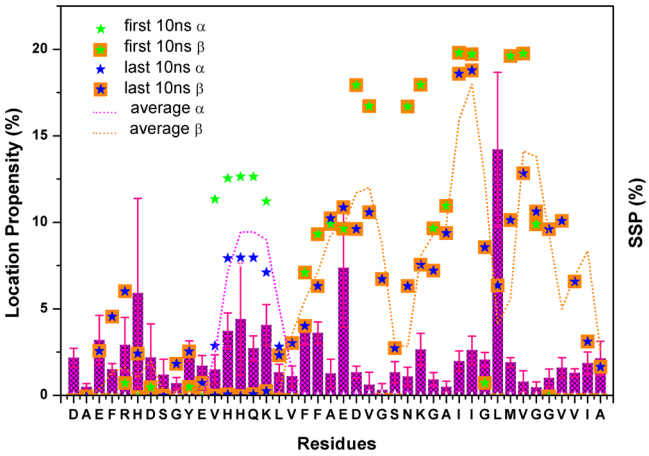

Figure 5. The plot gives the location propensity of curcumin on the Aβ dimer and the secondary structure propensity of Aβ. The heights of the purple bars are obtained by averaging over all trajectories that consist of the nearest residue of Aβ to curcumin. In addition, the helical structures (α-helix, 3-helix, and 5-helix) and β-sheet structures (β-sheet and β-bridges) are calculated for each of the 10 models at 4 ns intervals within a total simulation time of 500 ns. The structure propensity of the first 10 ns and the last 10 ns are then extracted from these results. The purple dotted line indicates the average α propensity of the residues during the whole simulation, and the orange dotted line indicates the β-sheet propensity of the residues. In addition, the green stars represents the secondary structure propensity for the first 10 ns, and the blue stars give the secondary structure propensity in the last 10 ns. Note that the stars are given an orange background to distinguish between the β- and the α-propensities.

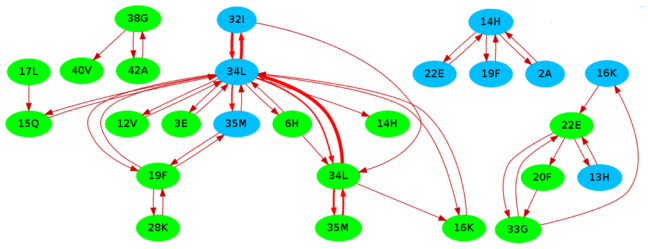

Figure 6. The common pathways of keto–enol curcumin over the Aβ dimer. Note that the blue circles represent residues from peptide A, and the green circles represent residues, those from peptide B. The thickness of the arrow indicates the level of popularity of the pathway. This figure is generated by the software Graphviz.

trajectories, we arrive at the common routes, which are shown in Figure 6. The most popular routes are: $34L_B \rightarrow 34L_A \rightarrow 32I_A \rightarrow 34L_A$ (14.5%), $34L_B \rightarrow 34L_A \rightarrow 34L_B \rightarrow 34L_A$ (9.6%), $34L_B \rightarrow 35M_B \rightarrow 34L_B \rightarrow 35M_B \rightarrow 34L_B$ (6%), and $32I_A \rightarrow 34L_A \rightarrow 35M_A \rightarrow 34L_A$ (4.8%). By examining this set of common pathways of curcumin, we see that residue 34L functions as a hub. Recall that 34L is also a popular dehydron (see Figure 4a) and recognition site on the Aβ.

The secondary structure propensity (SSP) for each Aβ residue was also analyzed (see Figure 5). We see that Val and Ile have a high propensity to form β-sheets. By comparing the SSP at the last 10 ns to the first 10 ns, we observe that the presence of curcumin perturbs the conformation of the Aβ secondary structure, resulting in a decrease in β-sheet secondary structure in the last 10 ns.

DISCUSSION AND CONCLUSION

The effect of curcumin on the stability of the Aβ dimer was examined by means of all-atom explicit solvent simulations. We found that curcumin plays the role of an efficient β-sheet breaker by reducing the number of residues adopting the β-sheet secondary structure. There are two possible reasons for its effectiveness. One reason could be due to the hydrophobicity of curcumin. Although curcumin has not been observed to penetrate and break the hydrophobic core of the Aβ dimer apart, the presence of curcumin near the Aβ proteins has perturbed and deformed the β-sheet secondary structure (see Figure 2). The other possible reason relates to the $\pi-\pi$ stacking interactions. This interaction is speculated to be critical for early molecular recognition and may serve to guide the formation of directionality in the self-assembly process.[53] Note that the polyphenol inhibitors are assumed to be directed to the amyloidogenetic core through specific aromatic interactions.[54] In this study, we have found that the π-stackings between the curcumin keto ring or enol ring with the Aβ aromatic rings exist throughout the whole simulation. Thus, we can perceive that the π-stacking interaction as well as the hydrophobic effects may play a non-negligible role in the inhibiting effects of curcumin on the Aβ peptides.

In addition, we have used the unwrapped amide-carbonyl hydrogen bonds to predict the potential ligand binding sites. Here, we have found that the amide-carbonyl hydrogen bonds of Val-24 and Asn-27, Glu-11 and Gln-15, Leu-34, and Ile-41, are very stable dehydrons. As curcumin approaches the Aβ dimer, the dehydrons of the dimer and the hydrophobic centers of curcumin form a complex due to the hydrophobic effect[65] based on a mechanism similar to the nanoscale dewetting transition.[66,67] Although the polar groups of curcumin can form hydrogen bonds with the dimer, the $\pi-\pi$ stacking interaction between the curcumin and the dimer partially immobilizes the aromatic arms of the curcumin and, hence, strengthen the hydrogen bond network between the two species. The contacts between curcumin and the Aβ proteins are dynamic, and the favorite curcumin location sites on Aβ are revealed. The common routes of curcumin as it travels around the Aβ dimer are analyzed. The curcumin molecules are observed to visit the residue Leu-34 regularly, and this residue can be treated as a hub within the common routes of curcumin. In conclusion, our study provides a detailed picture on the interaction of curcumin with the dimeric form of the Aβ oligomers.

ASSOCIATED CONTENT

Supporting Information

The contents of the supporting materials are (a) snapshots of the dimer at the end of the second set of simulation, (b) plots of the initial M0-M20 models, (c) calculated pK_a values for the titratable residues, (d) evolution of the Aβ secondary structure, (e) details of simulation system, (f) time evolution of the number of residues in β-structures and contact numbers, (g) the secondary structure propensity of Aβ residues in the presence and absence of curcumin, (h) the $\pi-\pi$ stacking propensity of Aβ residues, and (i) the occurrence of dehydron and the curcumin topology. This material is available free of charge via the Internet at http://pubs.acs.org.

AUTHOR INFORMATION

Corresponding Author

*E-mail: lockyue@ntu.edu.sg; ygmu@ntu.edu.sg.

dx.doi.org/10.1021/jp3034209 | J. Phys. Chem. B 2012, 116, 7428–7435

Notes

The authors declare no competing financial interest.

■ ACKNOWLEDGMENTS

The authors thank Hwee Jin Soh from the High Performance Computing Center for his kind help in the provision of computational support and Dr. Christopher M. Fraser from Bioanalytical Computing, L.L.C. for his generous help in data analysis. The authors thank the unknown reviewers, whose comments have substantially improved the quality of this paper. This work is supported in part by the IDA Cloud Computing Call for Project Proposals 2012, NTU Tier 1 Grant RG23/11, and the AcRF Tier 1 Grant RG52/08.

■ REFERENCES

(1) Karran, E.; Mercken, M.; Strooper, B. D. *Nat. Rev. Drug Discovery* **2011**, *10*, 698−712.
(2) Shankar, G. M.; Li, S. M.; Mehta, T. H.; Garcia-Munoz, A.; Shepardson, N. E.; Smith, I.; Brett, F. M.; Farrell, M. A.; Rowan, M. J.; Lemere, C. A.; et al. *Nat. Med.* **2008**, *14*, 837−842.
(3) Wang, Q.; Walsh, D. M.; Rowan, M. J.; Selkoe, D. J.; Anwyl, R. *J. Neurosci.* **2004**, *24*, 3370−8.
(4) Jang, H.; Zheng, J.; Lal, R.; Nussinov, R. *Trends Biochem. Sci.* **2008**, *33*, 91−100.
(5) Jang, H.; Arce, F. T.; Ramachandran, S.; Capone, R.; Lal, R.; Nussinov, R. *J. Phys. Chem. B* **2010**, *114*, 9445−9451.
(6) Jang, H.; Arce, F. T.; Ramachandran, S.; Capone, R.; Azimova, R.; Kagan, B. L.; Nussinov, R.; Lal, R. *Proc. Natl. Acad. Sci. U.S.A.* **2010**, *107*, 6538−6543.
(7) Jang, H.; Arce, F. T.; Ramachandran, S.; Capone, R.; Lal, R.; Nussinov, R. *J. Mol. Biol.* **2010**, *404*, 917−934.
(8) Shafrir, Y.; Durell, S.; Arispe, N.; Guy, H. R. *Proteins: Struct., Funct., Bioinf.* **2010**, *78*, 3473−3487.
(9) Sepulveda, F. J.; Parodi, J.; Peoples, R. W.; Opazo, C.; Aguayo, L. G. *PLoS One* **2010**, *5*, e11820.
(10) Geng, J.; Zhao, C.; Ren, J.; Qu, X. *Chem. Commun.* **2010**, *46*, 7187−7189.
(11) Huang, H.-C.; Lin, C.-J.; Liu, W.-J.; Jiang, R.-R.; Jiang, Z.-F. *Food Chem. Toxicol.* **2011**, *49*, 1578−1583.
(12) Atamna, H.; Boyle, K. *Proc. Natl. Acad. Sci. U.S.A.* **2006**, *103*, 3381−3386.
(13) Jiang, P.; Li, W. F.; Shea, J.-E.; Mu, Y. *Biophys. J.* **2011**, *100*, 1550−1558.
(14) Colombo, R.; Carotti, A.; Catto, M.; Racchi, M.; Lanni, C.; Verga, L.; Caccialanza, G.; Lorenzi, E. D. *Electrophoresis* **2009**, *30*, 1418−1429.
(15) Cohen, A. D.; Ikonomovic, M. D.; Abrahamson, E. E.; Paljug, W. R.; DeKosky, S. T.; Lefterov, I. M.; Koldamova, R. P.; Shao, L.; Debnath, M. L.; Mason, N. S.; et al. *Lett. Drug Des. Discovery* **2009**, *6*, 437.
(16) Scherzer Attali, R.; Pellarin, R.; Convertino, M.; Frydman Marom, A.; Egoz Matia, N.; Peled, S.; Levy Sakin, M.; Shalev, D. E.; Caflisch, A.; Gazit, E.; et al. *PLoS One* **2010**, *5*, e11101.
(17) Inbar, P.; Bautista, M. R.; Takayama, S. A.; Yang, J. *Anal. Chem.* **2008**, *80*, 3502−3506.
(18) Liang, G.; Li, X.; Chen, L.; Yang, S.; Wu, X.; Studer, E.; Gurley, E.; Hylemon, P. B.; Ye, F.; Li, Y.; Zhou, H. *Bioorg. Med. Chem. Lett.* **2008**, *18*, 1525−1529.
(19) Barry, J.; Fritz, M.; Brender, J. R.; Smith, P. E. S.; Lee, D.-K.; Ramamoorthy, A. *J. Am. Chem. Soc.* **2009**, *131*, 4490−4498.
(20) Ingolfsson, H. I.; Koeppe, R. E.; Andersen, O. S. *Biochemistry* **2007**, *46*, 10384−10391.
(21) Hatcher, H.; Planalp, R.; Cho, J.; Tortia, F. M.; Torti, S. V. *Cell. Mol. Life Sci.* **2008**, *65*, 1631−1652.
(22) Yoshida, H.; Okumura, N.; Nishimura, Y.; Kitagishi, Y.; Matsuda, S. *Exp. Ther. Med.* **2011**, *2*, 629−632.
(23) Balasubramanian, K. *J. Agric. Food Chem.* **2006**, *54*, 3512−3520.
(24) Yang, F.; Lim, G. P.; Begum, A. N.; Ubeda, O. J.; Simmons, M. R.; Ambegaokar, S. S.; Chen, P. P.; Kayed, R.; Glabe, C. G.; Frautschy, S. A.; et al. *J. Biol. Chem.* **2005**, *280*, 5892−5901.
(25) Garcia-Alloza, M.; Borrelli, L. A.; Rozkalne, A.; Hyman, B. T.; Bacskai, B. J. *J. Neurochem.* **2007**, *102*, 1095−1104.
(26) Varghese, K.; Molnar, P.; Das, M.; Bhargava, N.; Lambert, S.; Kindy, M. S.; Hickman, J. *J. PLoS One* **2010**, *5*, e8643.
(27) Ahmed, T.; Gilani, A.-H.; Hosseinmardi, N.; Semnanian, S.; Enam, S. A.; Fathollahi, Y. *Synapse* **2011**, *65*, 572−582.
(28) Park, S. Y.; Kim, D. S. *J. Nat. Prod.* **2002**, *65*, 1227−1231.
(29) Wang, L.; Li, C.; Guo, H.; Kern, T. S.; Huang, K.; Zheng, L. *PLoS One* **2011**, *6*, e23194.
(30) Lee, I.; Yang, J.; Lee, J. H.; Choe, Y. S. *Bioorg. Med. Chem. Lett.* **2011**, *21*, 5765−5769.
(31) Aggarwal, B. B.; Harikumar, K. B. *Int. J. Biochem. Cell Biol.* **2009**, *41*, 40−59.
(32) Ortica, F.; Rodgers, M. A. J. *Photochem. Photobiol.* **2001**, *74*, 745−751.
(33) Mague, J. T.; Alworth, W. L.; Payton, F. L. *Acta Crystallogr.* **2004**, *60*, 608−610.
(34) Payton, F.; Sandusky, P.; Alworth, W. L. *J. Nat. Prod.* **2007**, *70*, 143−146.
(35) Crescenzi, O.; Tomaselli, S.; Guerrini, R.; Salvatori, S.; D'Ursi, A. M.; Temussi, P. A.; Picone, D. *Eur. J. Biochem.* **2002**, *269*, 5642−5648.
(36) Gordon, J. C.; Myers, J. B.; Folta, T.; Shoja, V.; Heath, L. S.; Onufriev, A. *Nucleic Acids Res.* **2005**, *33*, 368−371.
(37) Myers, J.; Grothaus, G.; Narayanan, S.; Onufriev, A. *Proteins* **2006**, *63*, 928−938.
(38) Irwin, J. J.; Shoichet, B. K. *J. Chem. Inf. Model.* **2005**, *45*, 177−182.
(39) Schuttelkopf, A. W.; van Aalten, D. M. F. *Acta. Crystallogr. D* **2004**, *60*, 1355−1363.
(40) Olubiyi, O. O.; Strodel, B. J. *Phys. Chem. B* **2012**, *116*, 3280−3291.
(41) Hess, B.; Bekker, H.; Berendsen, H. J. C.; Fraaije, J. G. E. M. *J. Comput. Chem.* **1997**, *113*, 1463−1472.
(42) Nosé, S. *Mol. Phys.* **1984**, *55*, 255−268.
(43) Hoover, W. G. *Phys. Rev. A* **1985**, *31*, 1695−1697.
(44) Essmann, U.; Perera, L.; Berkowitz, M. L.; Darden, T.; Lee, H.; Pedersen, L. G. *J. Chem. Phys.* **1995**, *103*, 8577−8593.
(45) Sanner, M. F. *J. Mol. Graphics Model.* **1999**, *17*, 57−61.
(46) DeLano, W. L. *The PyMOL Molecular Graphics System*, Version 1.4, Schrödinger, LLC: 2011.
(47) Humphrey, W.; Dalke, A.; Schulten, K. *J. Mol. Graphics* **1996**, *14*, 33−38.
(48) Fraser, C. M.; Fernández, A.; Scott, L. R. *Technical Report TR-2011-05*; University of Chicago: Chicago, IL, 2011.
(49) Berendsen, H. J. C.; van Gunsteren, J. P. M.; Postma, W. F.; Hermans, J. *Intermol. Forces* **1981**, 331−342.
(50) Zhao, L. N.; Chiu, S.-W.; Benoit, J.; Chew, L. Y.; Mu, Y. *J. Phys. Chem. B* **2011**, *115*, 12247−12256.
(51) Ionov, M.; Klajnert, B.; Gardikis, K.; Hatziantoniou, S.; Palecz, B.; Salakhutdinov, B.; Cladera, J.; Zamaraeva, M.; Demetzos, C.; Bryszewska, M. *J. Therm. Anal. Calorim.* **2010**, *99*, 741−747.
(52) Zhao, L. N.; Long, H.; Mu, Y.; Chew, L. Y. *Int. J. Mol. Sci.* **2012**, *13*, 7303−7327.
(53) Gazit, E. *FASEB J.* **2002**, *16*, 77−83.
(54) Porat, Y.; Abramowitz, A.; Gazit, E. *Chem. Biol. Drug Des.* **2006**, *67*, 27−37.
(55) Scrutton, N. S.; Raine, A. R. *Biochem. J.* **1996**, *319*, 1−8.
(56) Hunter, C. A.; Sanders, J. K. M. *J. Am. Chem. Soc.* **1990**, *112*, 5525−5534.
(57) Xia, Z.; Zhu, Z.; Zhu, J.; Zhou, R. *Biophys. J.* **2009**, *96*, 1761−1769.
(58) Du, J.; Du, J.; Zhao, L.; Wang, L.; Liu, Y.; Li, D.; Yang, Y.; Zhou, R.; Zhao, Y.; Chai, Z.; et al. *Proc. Natl. Acad. Sci. U.S.A.* **2011**, *108*, 16968−16973.

(59) Zuo, G.; Gu, W.; Fang, H.; Zhou, R. *J. Phys. Chem. C* **2011**, *115*, 12322−12328.
(60) Fernández, A.; Scott, R. *Biophys. J.* **2003**, *85*, 1914−1928.
(61) Chen, J. P.; Zhang, X.; Fernandez, A. *Bioinformatics* **2007**, *23*, 563−572.
(62) Crespo, A.; Fernandez, A. *Mol. Pharm.* **2008**, *5*, 430−437.
(63) Fraser, C. M.; Fernández, A.; Scott, L. R. *Advances in Computational Biology*; Springer: New York, 2010; Chapter 53, pp 473−479.
(64) Betts, M. J.; Russell, R. B. *Bioinformatics for Geneticists*; Wiley: New York, 2003.
(65) Young, T.; Abel, R.; Kim, B.; Berne, B. J.; Friesner, R. A. *Proc. Natl. Acad. Sci. U.S.A* **2007**, *104*, 808−813.
(66) Liu, P.; Huang, X.; Zhou, R.; Berne, B. J. *Nature* **2005**, *437*, 159−162.
(67) Zhou, R.; Huang, X.; Margulis, C. J.; Berne, B. J. *Science* **2004**, *305*, 1605−1609.